

See discussions, stats, and author profiles for this publication at: <https://www.researchgate.net/publication/333073687>

Transfer and multitask learning using convolutional neural networks for buried wire detection from ground penetrating radar data

Conference Paper · May 2019

DOI: 10.1111/12.2518875

CITATIONS

0

READS

61

2 authors:



Enver Aydin

Hacettepe University

2 PUBLICATIONS 1 CITATION

SEE PROFILE



Seniha Yuksel

Hacettepe University

57 PUBLICATIONS 383 CITATIONS

SEE PROFILE

PROCEEDINGS OF SPIE

[SPIDigitalLibrary.org/conference-proceedings-of-spie](https://spiedigitallibrary.org/conference-proceedings-of-spie)

Transfer and multitask learning using convolutional neural networks for buried wire detection from ground penetrating radar data

Enver Aydin, Seniha Esen Yüksel Erdem

Enver Aydin, Seniha Esen Yüksel Erdem, "Transfer and multitask learning using convolutional neural networks for buried wire detection from ground penetrating radar data," Proc. SPIE 11012, Detection and Sensing of Mines, Explosive Objects, and Obscured Targets XXIV, 110120Y (10 May 2019); doi: 10.1117/12.2518875

SPIE.

Event: SPIE Defense + Commercial Sensing, 2019, Baltimore, Maryland, United States

Transfer and Multitask Learning using Convolutional Neural Networks for Buried Wire Detection from Ground Penetrating Radar Data

Enver AYDIN^{1,2}, Seniha Esen YUKSEL ERDEM¹,

¹Electrical & Electronics Engineering, Hacettepe University, Ankara, TURKEY

²ASELSAN, Ankara, TURKEY

ABSTRACT

In this work, plastic wires buried in dry, damp and wet soils are being detected from ground penetrating radar (GPR) images. Such detection is hard, mainly due to three facts: (1) detection of buried targets made of different materials but of the same shape is difficult from GPR images as their signatures look very similar; (2) the same object buried in different soils shows different signatures in a GPR image; and (3) obtaining GPR data in the millions range is not a viable option because of the difficulties in data collection. Therefore in this work, first, domain adaptation (DA) is used to bring the information from previously trained deep learning models on standard image processing tasks into the GPR domain. It is shown that with DA, high classification rates can be achieved even with small GPR datasets, and that these rates surpass the classification rates achieved by convolutional neural networks (CNNs). However, detecting the targets in different soils still remains a problem. Therefore, secondly, a multi-task CNN is proposed, in which, soil and target classification are stitched together. In doing so, our customized classifier detects targets according to soil type, and results in superior classification rates. To the best of our knowledge, we are the first group to use multi-task learning for buried target detection with GPR.

Keywords: GPR, Convolutional Neural Network, Domain Adaptation.

1. INTRODUCTION

Ground penetrating radar (GPR) can be described as a radar that aims to detect and identify objects subsurface [1]. Especially with the decrease in the metal content in most buried targets, GPR has been becoming the most dominant sensor for detection of buried objects with metal-free or small metal content [2]. Over the years, GPR has been quite often investigated in various fields including as oil, gas exploration, geology, canal and pipeline localization [3], but in particular for landmine detection [4]–[6].

Despite being the most popular method for detecting buried targets, GPR too has weaknesses. GPR systems need to dielectrically differentiate between soil and buried targets in order to detect buried targets. However, these differences are often not enough, which presents the biggest obstacle for a GPR system. If the dielectric difference is not large enough between the buried object and the lossy soil, target detection becomes especially hard [7]. Further, the detection performance depends not only on the properties of the buried targets, but also on the soil conditions, the temperature, weather conditions as well as the changing terrain. Typically, objects that are large and metallic are easier to detect when they are buried closer to ground surface, but will not be noticed if they are made from smaller, deeper buried and dielectric materials [8]. In addition, ground bounce and non-target reflections are more pronounced than buried object signatures, causing buried objects to become hard to notice. These negativities can lead to false alarms in target detection and can lead to dangerous consequences such as death or injury in the presence of explosives.

The research to decrease these false alarms range from developing new preprocessing methods to remove the ground bounce or clutters [5, 9, 10], to new detection algorithms [11, 12, 13], to sensor fusion [6, 14, 15]. However, all of these studies suffer from at least one of these problems, that the training data is not enough, and the extraction of features is very difficult and requires expert knowledge [16]. Based on the superiority of deep learning methods compared to traditional classification algorithms over many fields, and with the increase in the processing power of computers, these two issues have lately been addressed using deep learning algorithms in [17] and [18]. In [17], deep learning is used for the detection of buried pipes; and it is shown that the performance is only 83%, if the actual data is tested with a model trained by

synthetic data. If domain adaptation is applied, performance shifted up to 95%. The experimental results in this study confirm the idea that CNN can in principle be trained entirely from synthetic data.

One approach that is not considered in these studies is multi-task learning (MTL). MTL is a method in which multiple learning tasks are solved at the same time, and the useful information contained in one task is used to leverage the information contained in the second task. MTL; also called as participatory learning or as learning with auxiliary tasks; is being successfully used in several areas including natural language processing [19], speech recognition [20] and computer vision [21]. A shared property of these applications is that an additional task assists the main task through a common loss function with the goal of using field-specific knowledge in related tasks [22]. A nice overview of MTL methods can be found in [23]. For GPR, this field-specific knowledge, ie. the auxiliary task, can be the soil type or the humidity of the soil; as the soil properties greatly determine the shape and amplitude of the recorded signal.

In this paper, a deep-learning based transfer learning (TL) approach followed by multi-task learning (MTL) is proposed for the detection of buried wires that might indicate the existence of a nearby improvised explosive device. Detection of wires with GPR is a very under-studied topic; however, it can give significant clues when it is difficult to detect an improvised explosive device, which come in various sizes, forms and materials. For this purpose, first, synthetic data is generated with GPRMax [24]. In addition, a second dataset is obtained from the authors of [25]. Then, a Convolutional Neural Network (CNN) model is trained tailored for the dataset, until the performance reached a limit based on the parameters such as filters, order of layers and depth. However, it was seen that this performance can be increased and the evaluation time can be decreased if transfer learning is used.

Transfer learning is a method in which a pre-trained model for one task is reused as the starting point to learn a model for a second task [26]. If the images are from different domains, as in our case, where the first task is based on RGB image data whereas the second task is based on GPR data, TL is often referred to as domain adaptation. To train a better CNN model for GPR images, the first two layers (conv1, pool1, relu1, conv2, pool2, relu2) of Vggnet [27] were used as a feature extractor. Then, a third convolution layer and a fully-connected layer were added to these fixed layers and were trained on the GPR data. Although this method increased the detection rates, like many other classification algorithms, it lacked one pretty important information: GPR data is significantly affected from the type and the humidity of the soil. While a target placed in dry soil can be detectable, the same target may become almost invisible when the soil gets wet.

Finally, to take the soil type information into consideration, multi-task learning was proposed. In the proposed MTL framework, there is a two-network structure, one of which learns to discriminate the soil based on its humidity, and other which learns to identify the targets. These two networks are stitched together such that both tasks feed each other and result in improved prediction accuracy.

In the sections that follow, we first give information on the datasets we are using. Then, we provide a background on the CNN modules that form the backbone of our model; and complete it with domain adaptation and multi-task learning. Finally, we provide the experimental results and compare the algorithms on all datasets.

2. GPR DATASETS

Within the scope of this study, 3 different datasets have been studied. In the first dataset, plastic wire objects were placed in dry, damp and wet soil, and called as the target class. In the non-target class, non-plastic wires and irregular shaped objects were placed in dry, damp and wet soil. The dataset was divided into train, validation and test sets as shown in Table 1.

Table 1. Dataset I

Buried Material	TARGET			NON-TARGET					
	Wire (Plastic)			Wire (Non-plastic)			Irregular Shaped Objects		
Soil Moisture Level	Dry	Damp	Wet	Dry	Damp	Wet	Dry	Damp	Wet
Train	34	33	33	34	33	33	7	7	6
Validation	17	17	16	17	17	16	7	7	6
Test	17	17	16	17	17	16	7	7	6
Total	200			200			60		

The second dataset is generated to investigate the effect of the humidity in the soil on target detection, and to learn the soil types to aid in target detection. Therefore, dry, damp and wet soil classes were formed; in which the buried targets may or

may not exist. GPR scans of buried wires in different soil types are shown in Fig. 1. The amplitudes along the red lines in Fig. 1.(a,b,c) are plotted in Fig. 1.(d). It can be seen that for the same object, both the amplitude and the time of the return signals change, when it is put into different soils. In the time axis, 100 unit indicate 470ps.

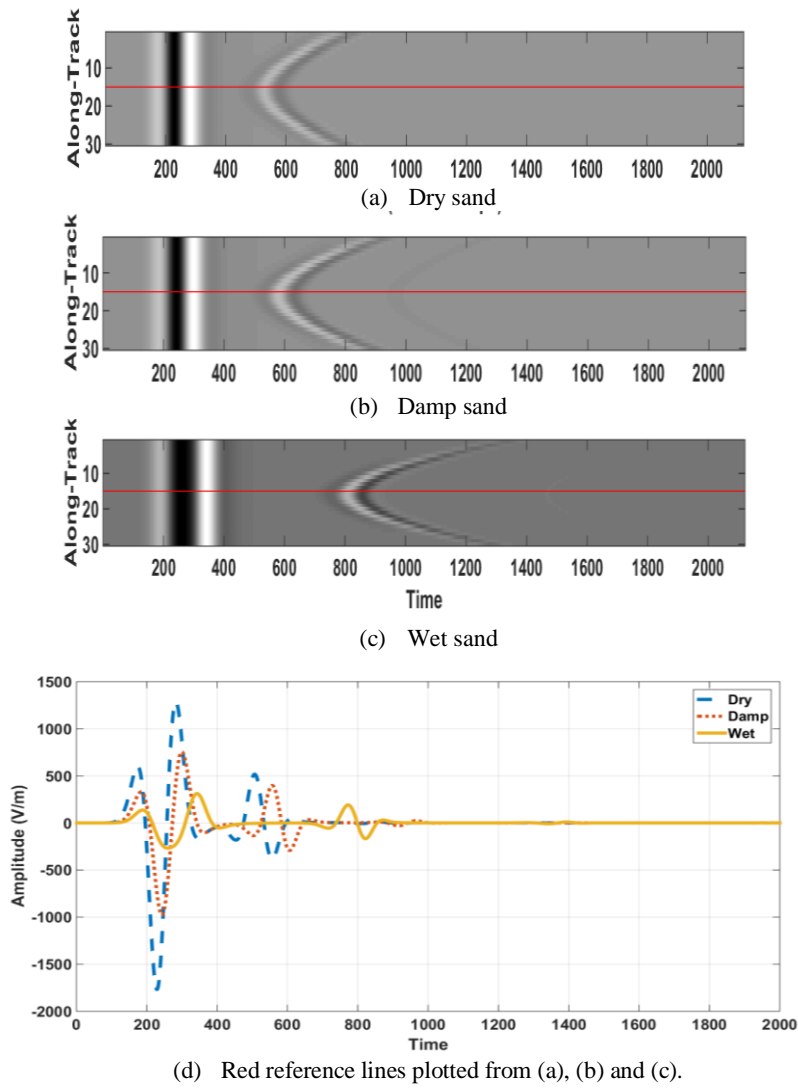


Fig. 1. GPR scans of buried wires

From now on, this dataset will be referred to as Dataset II, and the distribution of training, validation and test samples are shown in Table 2.

Table 2. Dataset II

Buried Material	Dry Soil		Damp Soil		Wet Soil	
	Wire	Irregular Shaped	Wire	Irregular Shaped	Wire	Irregular Shaped
Train	150	50	150	50	150	50
Validation	40	10	40	10	40	10
Test	70	30	63	47	42	34
Total	350		360		326	

Electromagnetic specifications of the materials used in the dataset are shown in Table 3. These specifications are relative permeability (μ_r), relative permittivity (ϵ_r) and conductivity (σ).

Table 3. Electromagnetic specifications of materials

Material	ϵ_r	σ	μ_r
Dry Sand	3	0.00001	2.0
Damp Soil	8	0.01	1.0
Wet Soil	20	0.1	1.0
Copper	10000	5600000	1
Concrete	6	0.001	1
Asphalt	2	0.01	2
Plastic	6	0.01	1

The electromagnetic simulation of the buried objects in various backgrounds are performed using Gprmax [24, 28], and these two datasets are generated according to the model shown in Fig. 2. Gprmax B-scan environment is modelled as 0.5 x 0.6 x 0.002 meters in along-track, depth and cross-track dimensions. Transmit (T) and receive (R) antenna pairs are separated by 4 cm. Ricker waveform at center frequency of 2.5 GHz is used in simulation. Objects are buried across in the cross-track dimension and at different depths notated as d as shown in Fig. 2. The buried wires have 5 - 10 - 15 mm radius denoted as r in the figure.

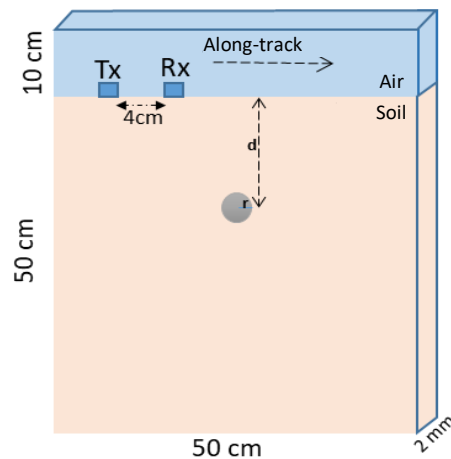
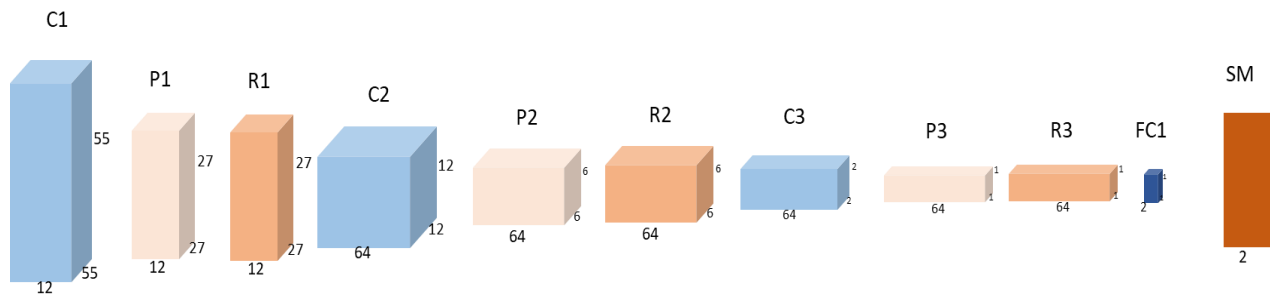


Fig. 2. Simulation environment for generated data

The third dataset is obtained from [25]. In this dataset, the simulation environment is modelled as 1 x 1 x 0.2 meters in cross-track, along-track and depth dimensions. T/R pairs are placed in the along-track direction, starting from 10 cm and going to 90 cm with 1cm steps; which result in 81 along-track positions. Transmit and receive antennas in a pair are separated by 2 cm. Soil depth is 15 cm and T/R pairs are placed 3 cm above the surface. Gaussian derivative waveform at center frequency of 2.5 GHz is used in simulation. The number of target and non-target objects are given in Table 4.

Table 4. Dataset III

	TARGET	NON-TARGET
Buried Material	Wire (PEC)	Stones And Clutters
Train	125	125
Validation	50	50
Test	50	50
Total	225	225



C: Convolutional Layer, P: Pooling Layer, R: ReLU Layer, FC: Fully Connected Layer, SM: Soft-max Layer

Fig. 3. Proposed Convolutional Neural Network Structure

The first dataset has been tested with three classification algorithms; namely; (i) standard deep convolutional neural networks, (ii) a deep learning model that uses transfer learning and (iii) a deep learning model that uses multitask learning in addition to TL. These will be explained in the sections that follow. The third dataset, however, does not have the humidity information. Therefore, only deep and transfer learning have been tested on the third dataset.

3. BACKGROUND ON CNNs

CNNs are like ordinary neural networks, in that they are made up of neurons that have learnable weights and biases. However, with the explicit assumption that the inputs are images, these weights can be shared, resulting in a big reduction in the amount of parameters and reduced complexity [29, 30, 31]. What makes CNNs desirable is that, both feature extraction and classification can be performed in a single network.

A CNN typically consists of the convolutional layers, rectification linear units (ReLU), pooling, and fully connected layers. The parameters of these layers, called the weights, are learned through backpropagation. Typically, the first layer learns more general attributes such as edge detection and color separation, whereas the next layers learn more special features. Each of the layers are described below:

Convolutional layer is made of filter banks and these filters are called as the weight matrix. Weight matrix consists of learnable parameters, which are learned through backpropagation using variable learning rates.

Activation layer is the nonlinearity in the network. It is applied after the convolutional layer and selects the larger values by comparing the current values with a certain value. In our network, we used the rectified linear unit (relu) activation function given in equation (1):

$$y = \max(0, x) \quad (1)$$

where x is the input and y is the output of the layer.

Pooling layer is applied to reduce the size of the matrix. It reduces the number of parameters by reducing the resolution, and reduces the probability of overfitting [30]. It is placed between convolutional layers and gradually reduces the number of parameters to alleviate the process load. Maximum and average pooling layers are the two most common pooling layers. In this work, maximum pooling was used.

Full-connected layer makes the high-level reasoning. Every neuron from the last pooling layer is connected to every layer of the fully-connected layer.

The CNN architecture used in this study is shown in Fig. 3. This serves as the baseline model, to which we compare our proposed methods.

4. PROPOSED METHOD

The framework of the proposed method is given in Fig. 4. where the first two layers are transferred from Vggnet, and the third convolutional layer is modified with a cross-stitching unit to perform multi-tasking. These are discussed in detail below.

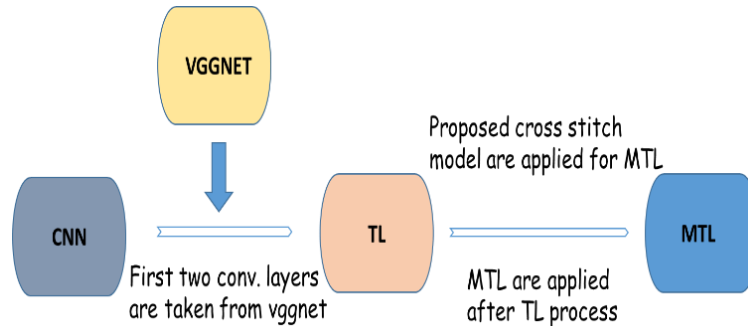


Fig. 4. The framework of the proposed method

For the CNN, the architecture was given in Fig. 3. Convolutional (C), pooling (P) and fully connected (FC) layers and their filter dimensions; depth, stride and zero padding values in proposed CNN architecture are shown in Table 5. Note that the GPR image dimensions are 227×227 pixels.

Table 5. Filters and Parameters Proposed in the CNN model

Layers	C1	P1	C2	P2	C3	P3	FC
Filter	11x11	3x3	5x5	2x2	4x4	2x2	1x1
Depth	12	12	64	64	64	64	2
Stride	4	2	2	2	2	2	1
Zero Padding	-	-	-	-	-	-	-

4.1 Transfer Learning

In this work, the imagenet-matconvnet-vgg-f model trained on the Imagenet Large Scale Visual Recognition Challenge (ILSVRC 2012) data [32] was used. The ILSVRC uses a portion of the ImageNet dataset, and consists of 1.2 million images collected from flickr and other search engines, and divided into 1000 categories. The Vggnet model trained on these images has 19 layers, consisting of 5 convolutional layers (together with some relu and pooling layers), before the fully-connected layers.

First, instead of training the CNN from scratch, we “transfer” the learned features from the first two convolutional layers of the Vggnet. In doing so, we treat the convolution layers as fixed feature extractors for our GPR dataset. We then train the third convolutional layer and the fully-connected layer, and fine tune the parameters for our wire-detection problem.

4.2 Multi-Tasking Learning

Multitasking learning is an approach that learns a task using the training information of other related auxiliary tasks. In this study, soil humidity was selected as the auxiliary task of buried target detection.

In order to use the proposed multitasking learning model, two single tasks, namely target detection and soil type detection, were trained separately. Then, these separate tasks were combined using a stitching coefficient. The goal of this unit is to get assistance from the soil type task for the target detection task. To provide this assistance, inspired by [33], a cross-stitching unit is placed between the two tasks. This unit combines the main task and the auxiliary task with a certain coefficient. The detailed illustration is shown in Fig. 5. Boxes shown with green color are convolutional layers and boxes filled with blue are pooling layers.

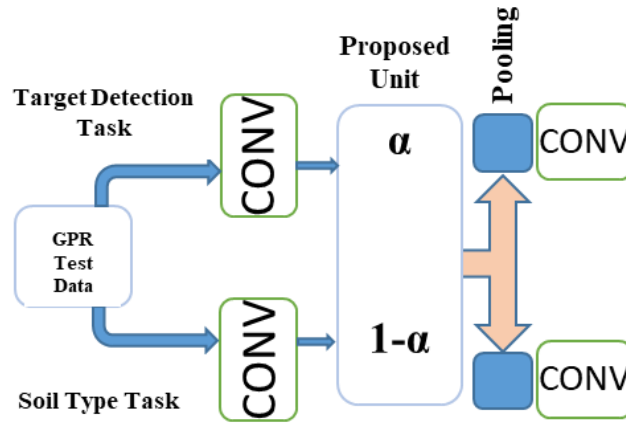


Fig. 5. Proposed Method Operation Scheme

The proposed cross-stitching unit added after the convolutional layer multiply the target task by the coefficient α and the auxiliary task by $(1-\alpha)$. For two different tasks as A and B, which are individually trained and modelled, we recommend an interface that will combine these two tasks. This unit will provide a linear combination of outputs after the convolutional layer as shown in equation (2):

$$[\tilde{x}] = [\alpha \quad (1 - \alpha)] \begin{bmatrix} x_A \\ x_B \end{bmatrix} \quad (2)$$

In this equation, x_A is the result of the convolutional layer before the cross stitch unit, and \tilde{x} is the result of the cross stitch unit operation. This output will generate input for the layers of the next A and B tasks. If this α value is chosen as '1', the single-task will be selected and the effect of the B task will be cancelled.

The value of α is learned during training. In the forward propagation, the formula of the feed-forward function is given in equation (2). For a gradient based back propagation [34], the partial derivative of the feed-forward layer is used. Backpropagation of the proposed cross stitching unit is defined in equations (3) and (4) by differentiating with respect to both the input matrix and α variable:

$$\frac{\partial L}{\partial x} = [\alpha \quad (1 - \alpha)] \begin{bmatrix} \frac{\partial L}{\partial \tilde{x}_A} \\ \frac{\partial L}{\partial \tilde{x}_B} \end{bmatrix} \quad (3)$$

$$\frac{\partial L}{\partial \alpha} = \frac{\partial L}{\partial \tilde{x}_A} x_A - \frac{\partial L}{\partial \tilde{x}_B} x_B \quad (4)$$

The expression L in equations describes the loss function in the course of the backpropagation process.

5. EXPERIMENTAL RESULTS

In the experiments, first, the data was pre-processed, then sent to the classifiers, each of which are explained below.

5.1 Pre-processing

The outputs of the electromagnetic simulation of the buried object model with Gprmax contain the ground bounce and clutter signals. To remove these undesired signals, a background removal was performed. The background was generated from the same soil in which no object is buried, and subtracted from the generated data. Further, the signature of the target shows diminishing image clarity proportional to the depth of the object, as shown in Fig.6 (a), where the signal level decreases towards the arms of the hyperbola shape formed by the target object. This is due to the trade-off between the signal level of reflections and the depth of the soil. To correct this behaviour, whitening is applied, which is a standard procedure and corrects for signal level differences [6, 15, 35, 36]. The result obtained by background removal and whitening is shown in Fig. 6. It can be seen that the decreasing signal level is corrected towards the hyperbola arms and the depth effect is removed.

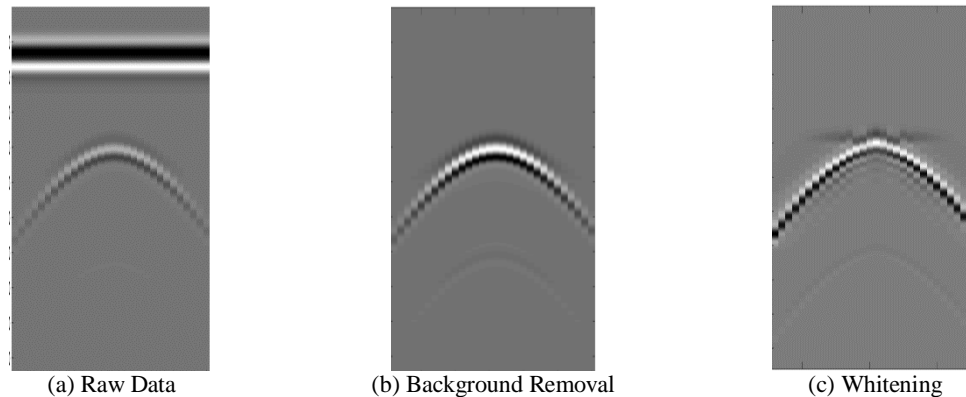


Fig. 6. Pre-processing Results.(a) The raw data shows the ground bounce and the signal decrease based on depth. (b) Ground bounce is removed through background subtracting. (c) Whitening increases the signal at the arms of the hyperbola.

5.2 Classification Results

Transfer and multitask learning methods are applied on the first, second and third datasets, and the experimental results are given in Table 6. In Table 6, the main task is set as the target detection task, and the auxiliary task is selected to be the soil classification task. The classification was run 25 times for each task, and the mean and standard deviation values were reported. In Table 5, the baseline CNN resulted in 74.1% accuracy in target detection, which increased to 77.4% with TL, and to 78.59% with MTL on the target detection dataset I. Therefore, it can be seen that both TL and MTL gradually increased the classification rates. On the second dataset, soil classification accuracy was computed, and it was found to be 58.6% with the baseline CNN, which increased to 76.9% with transfer learning. On the third dataset, target detection accuracy was 91.5% with baseline CNN, which increased to 91.7% with TL. Unfortunately, there is no wet/damp/dry soil for the third dataset, ie. all the targets are buried in one type of soil humidity; therefore, we could not compute the MTL scores.

Table 6: Experimental Results Comparing Baseline CNN, Transfer Learning and Multitask Learning

Classification Accuracy	CNN		TL		MTL	
	μ	σ	μ	σ	μ	σ
Target Detection (Dataset I)	74,1	0,5	77,4	2,2	78,59	1.73
Soil Detection (Dataset II)	58,6	2,8	76,9	2,0	-	-
Target Detection (Dataset III)	91,5	1,5	91,7	1,5	-	-

Three interesting runs of multitask learning are given explicitly in Table 7. In the first row, the target classification task on the first dataset is reported as 77.50%; and the soil classification on the second dataset is reported as 76.92% using TL. Then, cross-stitching finds the optimal value of α to be 0,7682. With stitching, the classification accuracy on the first dataset is increased to 79.17%. In the third row, again the target task is increased from 75% to 76.67%. However, a very interesting result is seen in the second row: the target classification accuracy is already high; therefore, the value of α is found to be 1; indicating that the soil task is not contributing to the classification in MTL. Therefore, if the auxiliary task is not found to be benefitting the main task, it receives a zero weight, and does not affect the classifier.

Since there are both plastic target wires and non-plastic non-target wires exist in the first dataset, the results are pretty hard to interpret. Nonetheless, below, we give the GPR images that are correctly and incorrectly classified, in Fig. 7.

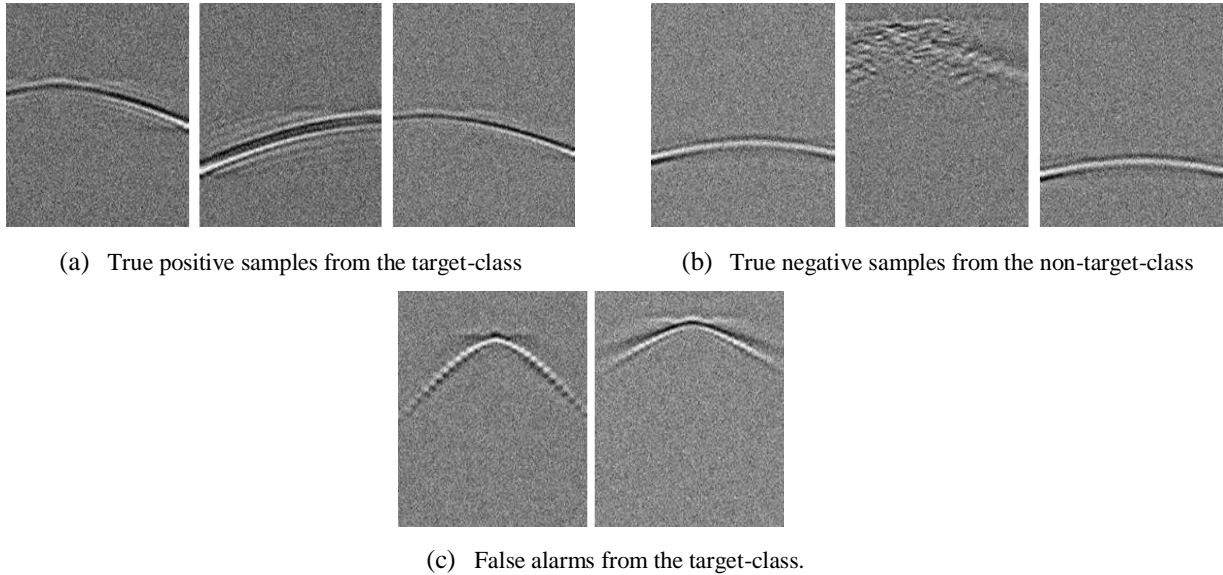
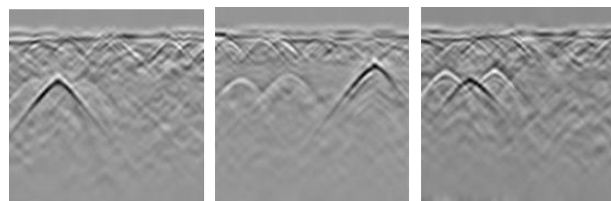


Fig. 7. Correctly and incorrectly classified samples from Dataset I.

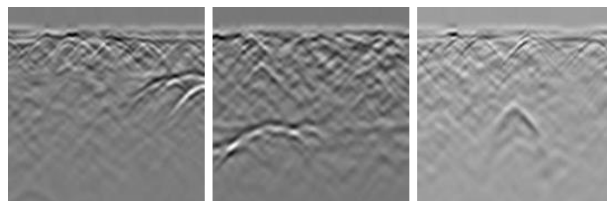
For the third dataset, CNN and TL was applied, and some sample results are given in Fig. 8 and 9. When we examine the results, it is seen that high contrast reflections from buried PEC wires are easy to detect in the target class. However, if clutter objects had strong signatures, they were classified as false alarms, as expected.

Table 7. Experimental results showing the details of multitask learning.

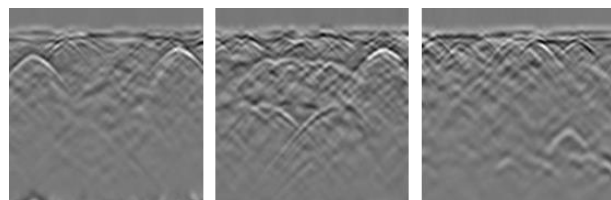
<i>Task: Learning</i>	<i>Accuracy</i>		<i>Source Task</i>		α
	μ	σ	<i>Target</i>	<i>Soil</i>	
Target: Multitask I	79,17	-	77,50	76,92	0,7682
Target: Multitask II	80,00	-	80,00	76,92	1
Target: Multitask III	76,67	-	75,00	76,92	0,8705



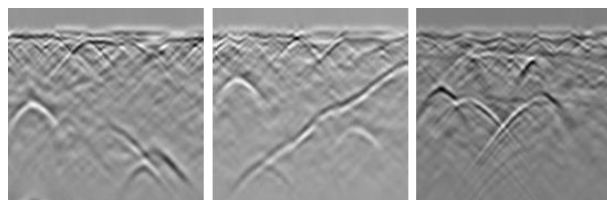
(a) True positive samples from the target-class



(a) False alarm in target-class



(b) True negative samples from the non-target-class



(b) False alarm in non-target-class

Fig. 8. Correct classification samples from Dataset III.

Fig. 9. False alarm samples from Dataset III.

6. CONCLUSION

Buried wire detection with GPR is an important problem in fighting with improvised explosive devices. In this study, synthetically generated wire data was classified using three proposed approaches: (i) a baseline CNN model, (ii) transfer learning from the Vggnet, and (iii) a multi-task model. Over repeated experiments, it was shown that the transfer learning increased the classification rates when compared to the CNN; and MTL increased them even further. This shows that the humidity of the soil is a good auxiliary task which should be used in target detection from GPR. Another interesting observation with MTL was that where the multitask learner failed to increase the performance, the α values was set to '1' and showed that the best performance was in the target task.

REFERENCES

- [1] Leon, L. P., Young, J. D. and Daniels, J. J.: "Ground Penetrating Radar as a Subsurface Environmental Sensing Tool," *Proceedings IEEE*, vol. 82, no. 12, pp. 1802–1822, 1994.
- [2] Yuksel, S. E. and Gader P. D.: "Context-based Classification Using a Mixture of Hidden Markov Models with Applications in Landmine Detection," *IET Computer Vision*, pp. 873 - 883, vol. 10, issue: 8, 2016.
- [3] Benedetto, A., Tosti, F., Ciampoli L., Amico F. D.: "GPR Applications Across Engineering and Geosciences Disciplines in Italy: A Review," *IEEE Journal of Selected Topics in Applied Earth Observations and Remote Sensing*, Volume: 9, Issue: 7, July 2016.
- [4] Wilson, J. N., Gader, P., Member S., Lee, W.-H., Frigui, H., and Ho, K. C.: "A Large-Scale Systematic Evaluation of Algorithms Using Ground-Penetrating Radar for Landmine Detection and Discrimination," *IEEE Transactions on Geoscience and Remote Sensing*, vol. 45, no. 8, pp. 2560–2572, 2007.
- [5] Zhu, Q. and Collins, L. M.: "Application of feature extraction methods for landmine detection using the Wichmann/Niitek ground-penetrating radar," *IEEE Transactions on Geoscience and Remote Sensing*, vol. 43, no. 1, pp. 81–85, 2005.
- [6] Stanley, R. J., Gader, P. D. and Ho, K. C.: "Feature and decision level sensor fusion of electromagnetic induction and ground penetrating radar sensors for landmine detection with hand-held units," *Information Fusion*, vol. 3, no. 3, pp. 215–223, 2002.
- [7] Vitebskiy, S. and Carin, L.: "Resonances of perfectly conducting wires and bodies of revolution buried in a lossy dispersive half-space," *IEEE Transactions Antennas Propagation*, vol. 44, no. 12, pp. 1575–1583, 1996.
- [8] Dogan, M., Gumus, S. and Turhan-Sayan, G.: "Detection of conducting and dielectric objects buried under a layer of asphalt or concrete using simulated ground penetrating radar signals," in *International Conference on Electromagnetics in Advanced Applications (ICEAA)*, pp. 1535–1538, 2017.

- [9] Baydar, B., Akar, G. B., Yuksel, S. E. and Ozturk S.: "Fusion of KLMS and blob based pre-screener for buried landmine detection using ground penetrating radar," SPIE Defence and Security, Baltimore, USA vol. 9823, p. 98231D-9823-7, 2016.
- [10] Singh, N. P. and Nene, M. J.: "Buried object detection and analysis of GPR images: Using neural network and curve fitting," 2013 Annual International Conference on Emerging Research Areas and 2013 International Conference on Microelectronics Communications and Renewable Energy, Kanjirapally, pp. 1-6, 2013.
- [11] Pasolli, E., Melgani, F., and Donelli, M.: "Automatic analysis of GPR images: A pattern-recognition approach," IEEE Transactions on Geoscience and Remote Sensing, vol. 47, no. 7, pp. 2206-2217, 2009.
- [12] Sakaguchi, R., Morton, K.D., Collins, L.M., Torrione P.A.: "A comparison of feature representations for explosive threat detection in ground penetrating radar data," IEEE Transactions on Geoscience and Remote Sensing 55 (12), 6736-6745, 2017.
- [13] Zhang, X., Bolton, J., Gader, P.: "A new learning method for continuous hidden Markov models for subsurface landmine detection in ground penetrating radar", IEEE Journal of Selected Topics in Applied Earth Observations and Remote Sensing, vol. 7, issue 3, pp. 813-819, 2014.
- [14] Yuksel, S.E., Akar, G.B., Ozturk, S.: "Fusion of forward-looking infrared camera and down-looking ground penetrating radar for buried target detection," Proc. SPIE 9454, Detection and Sensing of Mines, Explosive Objects, and Obscured Targets XX, 945418, 21 May 2015.
- [15] Smith, R.E., Anderson, D.T., Ball, J.E., Zare, A., Alvey, B.: "Aggregation of Choquet integrals in GPR and EMI for handheld platform-based explosive hazard detection," Detection and Sensing of Mines, Explosive Objects, and Obscured Targets XXII, vol. 10182, pp. 1018217, 2017.
- [16] Yuksel, S. E., Bolton, J. and Gader P.: "Multiple-Instance Hidden Markov Models With Applications to Landmine Detection," IEEE Transactions on Geoscience and Remote Sensing vol. 53, no. 12, pp. 6766-6775, 2015.
- [17] Lameri, S., Lombardi, F., Bestagini, P., Lualdi, M. and Tubaro, S.: "Landmine Detection from GPR Data Using Convolutional Neural Networks," 25th European Signal Processings Conference, pp. 538-542, 2017.
- [18] Bralich, J., Reichman, D., Collins, L. M. and Malof, J. M.: "Improving convolutional neural networks for buried threat in ground penetrating radar using transfer learning via pre-training," in SPIE Defense and Security. International Society for Optics and Photonics, pp. 101820X, 2017.
- [19] Collobert, R. and Weston, J.: "A unified architecture for natural language processing," in Proceedings of the 25th international conference on Machine learning - ICML '08, 2008, pp. 160-167.
- [20] Deng, L., Hinton, G., and Kingsbury, B.: "New types of deep neural network learning for speech recognition and related applications: an overview," in 2013 IEEE International Conference on Acoustics, Speech and Signal Processing, 2013, pp. 8599-8603.
- [21] Girshick, R.: "Fast R-CNN," in Proceedings of the IEEE International Conference on Computer Vision, 2015, vol. 2015 Inter, pp. 1440-1448.
- [22] Caruana, R.: "Multitask Learning," Machine Learning, vol. 28, no. 1, pp. 41-75, 1997.
- [23] Ruder, S.: "An Overview of Multi-Task Learning in Deep Neural Networks", arXiv preprint arXiv:1706.05098, 2017.
- [24] Warren, C., Giannopoulos, A. and Giannakis I.: "An advanced GPR modelling framework: The next generation of gprMax," 2015 8th International Workshop on Advanced Ground Penetrating Radar (IWAGPR), Florence, 2015, pp. 1-4.
- [25] Yilmaz, U.: "Buried Wire Detection Using Ground Penetrating Radars", Masters Thesis, Middle East Technical University, Ankara, Turkey, 2017.
- [26] Ren, H., Kanhabua, N., Mogelmose, A., Liu, W., Kulkarni, K., Escalera, S., Baro, X., Moeslund, T.B.: "Back-dropout transfer learning for action recognition, IET Computer Vision, vol. 11, issue 6, p. 696 - 702, 2017.
- [27] Chatfield, K., Simonyan, K., Vedaldi, A., Zisserman, A.: "Return of the Devil in the Details: Delving Deep into Convolutional Nets", British Machine Vision Conference, 2014.
- [28] Warren, C., Giannopoulos, A. and Giannakis, I. I.: "gprMax: Open source software to simulate electromagnetic wave propagation for Ground Penetrating Radar", Computer Physics Communications, 209, 163-170, 2016.
- [29] Rosenblatt, F.: "The perceptron: A probabilistic model for information storage and organization in the brain.," Psychological Review, vol. 65, no. 6, pp. 386-408, 1958.
- [30] Karpathy, A.: "Convolutional Neural Networks for Visual Recognition," Stanford CS class CS231n notes, [Online]. Available: <http://cs231n.github.io/transfer-learning/>. [Accessed: 01-Oct-2017], 2017.
- [31] Yosinski, J., Clune, J., Bengio, Y. and Lipson, H.: "How transferable are features in deep neural networks?," Advances in Neural Information Processing Systems 27, pp 3320-3328, 2014.

- [32] Russakovsky, O., Deng, J., Su, H., Krause, J., Satheesh, S., Ma, S., Huang, Z., Karpathy, A., Khosla, A., Bernstein, M., C. Berg, A. and Fei-Fei, L.: "ImageNet Large Scale Visual Recognition Challenge". IJCV, 2015
- [33] Misra, I., Shrivastava, A., Gupta, A. and Hebert, M.: "Cross-stitch Networks for Multi-task Learning," arXiv:1604.03539, 2016.
- [34] LeCun, Y., Bottou, L., Bengio, Y. and Haffner, P.: "Gradient Based Learning Applied to Document Recognition," Proc. IEEE, vol. 86, no. 11, pp. 2278–2324, 1998.
- [35] Aydin, E. and Yuksel, S. E.: "Buried target detection with ground penetrating radar using deep learning method," in 2017 25th Signal Processing and Communications Applications Conference (SIU), 2017, pp. 1–4.
- [36] Aydin, E. and Yuksel, S. E.: "Transfer and Multitask Learning Method for Buried Wire Detection via GPR," in 2018 26th Signal Processing and Communications Applications Conference (SIU), 2018, pp. 1–4.